MRS Advances (2023) 8:148–151
https://doi.org/10.1557/s43580-023-00546-w

ORIGINAL PAPER

Antenna-coupled graphene josephson-junction terahertz detector

F. Javier Gonzalez[1] · Michael S. Lodge[2] · Masahiro Ishigami[2,3] · Richard A. Klemm[2] · Ami Rathod[2] · Kirsten L. Lina[2] · Anna C. Bowman[2] · Francisco Hernandez[2] · Chris J. Fredricksen[1] · Coleman Cariker[1] · R. E. Peale[1,2]

Received: 17 November 2022 / Accepted: 13 March 2023 / Published online: 22 March 2023

Abstract

Highly sensitive, broadly tunable detectors are needed for future sensing applications and quantum information systems. A promising material for these challenges comprises stacked graphene sheets having a "magic" twist angle between their in-plane symmetry axes. This material displays superconductivity with a ~ 2 K transition temperature. We investigate a proposed design for a fast and sensitive detector of THz and mm-waves based on antenna-coupled magic-angle-twist-graphene Josephson junctions. The considered non-bolometric detection mechanism depends on the decrease in the maximum zero-voltage DC current when AC current is driven through the junction. Finite element electrodynamic simulations favor the bowtie over log-periodic, square spiral, and Archimedean spiral antenna designs. Responsivity, noise-equivalent-power, and the prospects for single-photon detection are estimated.

Introduction

Emerging 5G and 6G (mm-wave to THz) technologies offer an interesting new spectral domain for quantum communication and cryptography, which often demand both single-photon sensitivity and high speed [1]. A single-photon detector of mm-waves to low-THz has been suggested recently for this application [2]. An opportunity for a fast and sensitive THz to mm-wave detector is a "video"-mechanism [3] antenna-coupled, magic-angle-twist-graphene superconducting Josephson junction (JJ) [4]. JJs also have a bolometric detection mechanism, which can be very sensitive, but the video-mechanism has "very great speed advantage over the bolometer" [3]. A superconducting "magic angle twisted bilayer graphene" bolometer without a JJ detected via the temperature dependence of the critical current [5]. JJ bolometers using non-superconducting-graphene as the weak link between conventional superconductors have demonstrated single-photon sensitivity [6–10]. In contrast, this paper considers a detector based on the video (non-bolometric) mechanism in a JJ-based entirely on superconducting-graphene. The potential speed advantage of the video- over bolometric-mechanism may have advantage for quantum cryptography at high-bit-rate [11].

A "magic" twist angle between graphene sheets flattens the electronic band structure near the Dirac point, creating a high density of states and the possibility of superconductivity [12]. The superconducting transition temperature is ~ 2 K for 2–4 layers, and superconducting-graphene JJs have been demonstrated [12]. This paper considers the possibility of creating ultrasensitive detectors of THz and mm-waves by coupling such JJs to antennas. Figure 1 (left) presents a schematic of the proposed device design. Superconductivity in the magic-angle-twist graphene is achieved by suitable gating. The JJ normal weak link is achieved by different localized gating. Hexagonal boron nitride (hBN) is the gate dielectric. DC current bias through the JJ is sourced through the antenna (Source and Drain) while measuring the DC voltage. The antenna collects THz/mm-wave radiation and sources the associated AC current to the JJ at the feed.

Antennas collect THz/mm-wave radiation with an effective area that is orders of magnitude larger than any possible graphene sensing element at the antenna feed. By definition, absorption is 100% for radiation that falls within an antenna's effective area [13], while the absorption of graphene itself is thought to be less than 10% [5]. The excited antenna currents are concentrated in the JJ load, thus amplifying the AC voltage across the JJ that is responsible for the video

✉ R. E. Peale
robert.peale@ucf.edu

[1] Truventic LLC, 1209 W. Gore St., Orlando, FL 32816, USA

[2] Physics Department, University of Central Florida, Orlando, FL 32816, USA

[3] Nanoscience Center, University of Central Florida, Orlando, FL 32816, USA

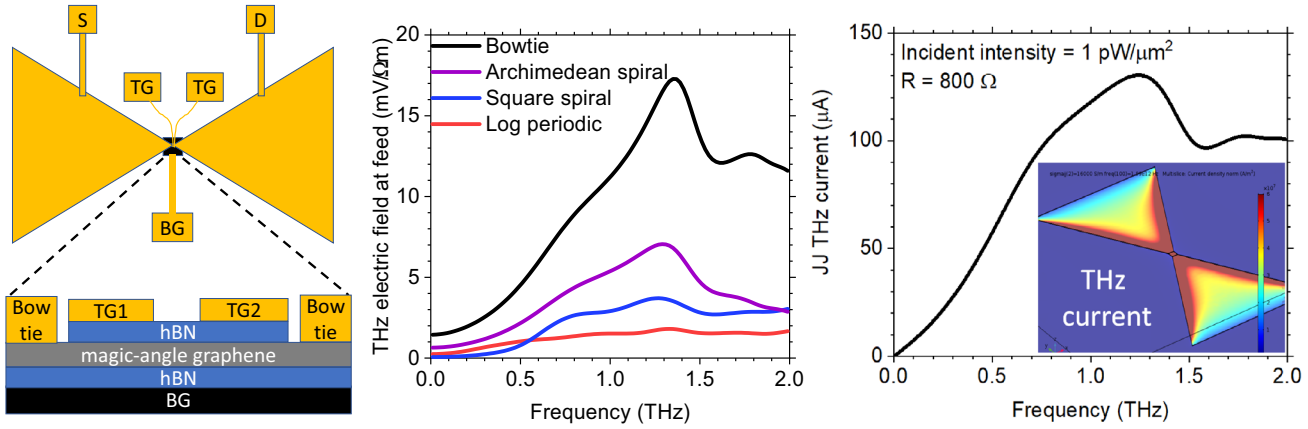

Fig. 1 (left) Schematic of proposed detector design, showing top view with bowtie antenna and side view showing layers. Relative dimensions are not to scale. *S* source, *D* drain, *TG* Top gate, *BG* Back gate, *hBN* Hexagonal boron nitride. (center) COMSOL simulations of electric field at the feed for various antenna designs with no load. (right) COMSOL simulation of current for bowtie antenna with 800 Ω load and 1 pW/μm^2 incident intensity. (inset) Current distribution in the bowtie, which has 80 μm length

detection mechanism. Antennas also provide wavelength and polarization selectivity [14]. They are easily fabricated into arrays and may be combined in series or parallel to enhance DC output voltage or current, respectively. The antenna function is largely independent of temperature, and it is accurately predicted by numerical electrodynamic simulations. Antenna coupling separates collection and detection functions, so that each can be independently optimized [13].

Results

Figure 1 (center) compares COMSOL simulations of open-circuit voltage at the antenna feed for four different antenna designs [14]. A THz resonance is observed, and the bowtie gives the highest AC voltage. Figure 1 (right) presents the current through an 800 Ω load at the feed of a bowtie antenna for 1 pW/μm^2 incident intensity. The inset shows the calculated AC current distribution in the antenna and its concentration at the feed.

Figure 2 (left) presents JJ Voltage-Current (VI) curves replotted from [12]. In the video detector mechanism, the maximum zero-voltage-current I_1 (JJ switching current) is depressed when an AC voltage appears across the JJ. Such a voltage appears when an AC current is driven through a JJ load, sourced by an antenna, because the AC impedance of the JJ is non-zero even when the DC resistance is zero. The device is current biased at the dark value of I_1. When mm-waves or THz are absorbed by a suitable antenna with the JJ at its feed, I_1 shifts below the bias point, and a DC voltage appears across the JJ. The sensitivity of the video detection mechanism depends on the dynamic resistance (steepness) of the VI curve at the bias point.

The I_1 value shifts similarly with increasing temperature (Fig. 2), giving rise to the bolometric-mechanism, which can be very sensitive. For such thermal detectors, speed is

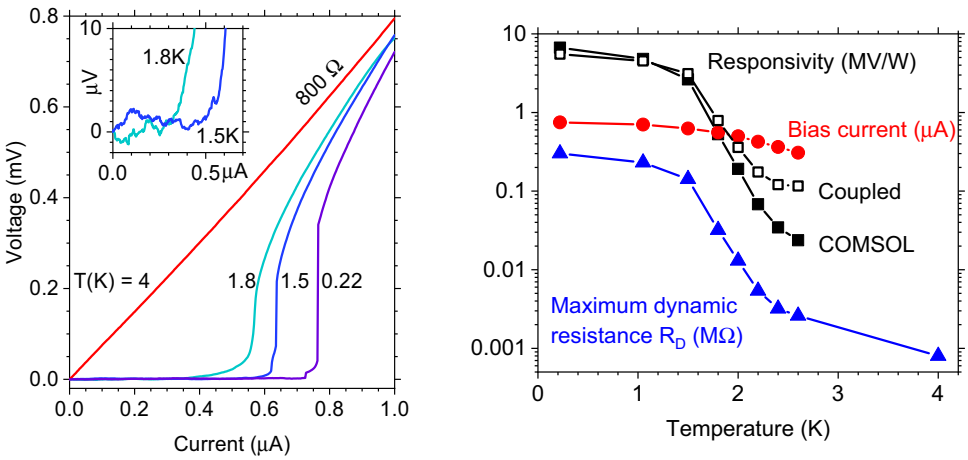

Fig. 2 (left) Voltage-current curves for superconducting-graphene Josephson junction from ref. [12]. JJ temperatures are indicated next to each curve. The inset is a blow-up to reveal the ~ 1 μV noise level. (right) Temperature dependence of optimum DC current bias, dynamic resistance at the bias point, and responsivity calculated by numerical (COMSOL) and analytical (Coupled) methods

determined by the thermal time-constant, which is short for graphene due to its small heat capacity. However, the non-bolometric "video" mechanism is thought to be faster and still very sensitive [3]. Experimentally, excellent thermal grounding could suppress a bolometric contribution to a video detector.

The resistively shunted junction (RSJ) model for JJ detectors comprises an ideal junction with only pair tunnelling current and a parallel shunt resistor R that carries only quasiparticle current. The value of R is the normal state resistance [3], which according to Fig. 2 (left) is 800 Ω. THz photon energies exceed the superconducting gap, so THz currents pass mainly through R. Additional inductive reactance determined from the Josephson equations [3] depends on AC current, so its estimation is complicated. We assume R, the lower bound on impedance, for our responsivity estimates.

The shift $\delta I_1 = -\left(2eV_{THz}/\hbar\omega\right)^2 I_1/4$ according to [3]. The squared factor is the ratio of the pair energy difference on the two sides of the junction to the photon energy. We assume the detector is DC current biased at I_1, which we take to be the point with the maximum dynamic resistance $R_D = dV/dI$. R_D and I_1 are found from the DC transport curves Fig. 2 (left) and are plotted as function of temperature in Fig. 2 (right). The shift results in a DC output voltage $\delta V_{out} = R_D \delta I_1$, and this response is proportional to absorbed power. With impedance mismatch between antenna and load already accounted for in the COMSOL simulation, the maximum $I_{THz} = 130$ μA (Fig. 1, right), gives an absorbed power $I_{THz}^2 R = 13.5$ μW at 1.25 THz. The temperature dependence of the responsivity (δV_{out} / absorbed power) is plotted as solid black symbols in Fig. 2 (right) and labeled "COMSOL". The maximum value is 7 MV/W. Responsivity is ~ 10 × smaller at T = 1.7 K than at 0.3 K.

Alternatively, the *coupled* power responsivity for a JJ detector is $S = R_D/2I_1 R\ \Omega^2$, where πΩ approximately equals the ratio of photon energy to gap [3]. At 1.25 THz, Ω ~5. The impedance of the bowtie acting as a current source is 300 Ω at the 1.25 THz resonance, so that it will couple 55% of the absorbed optical power to an 800 Ω load at its feed. Accounting for this mismatch, we obtain the responsivity curve given by open square symbols in Fig. 2 (right) and labeled "coupled". The results agree well with those of the COMSOL simulation over most of the temperature range. Since the impedance of a bowtie can be adjusted by changing its shape, responsivity can be improved.

By expanding the V-I data from [12], we find the broad-spectrum noise amplitude to be ~ 1 μV, as shown in the inset of Fig. 2 (left). Thus, the noise-equivalent-power (NEP) is not worse than 0.14 pW. It would be much smaller (better) if we restricted the noise spectral bandwidth to just 1 Hz, as is usually done via lock-in detection. An NEP of 0.14 pW, corresponds to a photon flux at 1.25 THz of ~ 1 photon every 6 ns. The prospects for single-photon detection seem good.

Fabrication and characterization

Device fabrication first builds a magic angle graphene stack, fully encapsulated with hexagonal boron nitride (hBN) flakes, using a cut-and-stack method described in [5]. We use pyramidal polydimethylsiloxane (PDMS, Sylgard 180) stamps having ~ 180 μm plateau edge length. We use poly(bisphenol A carbonate) (PC) film as a sacrificial interface layer between the hBN and the PDMS [15]. The 20–80 nm thick hBN encapsulating flakes serve as gate dielectrics. Fabrication has been completed this far. Next, the stack will be transferred onto a prefabricated gold/chromium back gate and heated to 175 °C to melt the PC film, detaching it from the PDMS. The device chip will then be cooled, removed from the transfer station, and gently soaked in chloroform to dissolve the PC residue. Next, we will apply bottom-gate contacts and top gates by electron-beam lithography for bias control of the Fermi level and creation of the JJ weak link, respectively. Bowtie antennas will be fabricated by contact photolithography with the stack placed at the feed of the antenna.

We will first measure the DC and rf electronic properties of the magic angle graphene and JJ in a 40 mK cryostat. Optical measurements will be performed using a Janis 8DT cryostat with immersion in pumped superfluid He at 1.7 K. The source will be a backward wave oscillator (Microtech Instruments) tunable from 160 GHz to 1.4 THz. For THz characterization in the 40 mK cryostat, which lacks external optical access, we plan to use a thermal source with THz bandpass filter filtering [16].

Summary

We considered an antenna-coupled Josephson junction video detector entirely fabricated from superconducting-graphene, in contrast to the well-studied JJ bolometers that use a normal graphene weak link between conventional superconductors [6–10]. The video detection mechanism is expected to be faster than the bolometric-mechanism [3]. Hence, the considered detector may have advantages for certain applications, such as high-bit-rate quantum communication and cryptography [11]. Responsivity, noise-equivalent-power, and noise-equivalent-photon flux for the considered design were estimated using published voltage-current curves [12], numerical calculations, and analytical theory. The estimate suggests that the device has the potential to detect single-photons.

Acknowledgments This work was supported by Army OSD STTR contract #W911NF22P0026.

Funding U.S. Army, W911NF22P0026, F. Javier Gonzalez

Data availability Truventic holds data rights under its STTR contract, but data are available from the authors upon reasonable request.

Declarations

Conflict of interest R. E. Peale and C. J. Fredricksen have ownership in Truventic and may benefit financially from the results of this research. Otherwise, all authors certify that they have no affiliations with or involvement in any organization or entity with any financial interest or non-financial interest in the subject matter or materials discussed in this manuscript.

References

1. M.D. Eisaman, J. Fan, A. Migdall, S.V. Polyakov, Invited review article: single-photon sources and detectors. Rev. Sci. Instr. **82**, 071101 (2011). https://doi.org/10.1063/1.3610677
2. V.F. Guedes, F.A. Mendonca, J.B.R. Silva, R.V. Ramos, Discrete variable quantum key distribution in millimeter-wave and THz regions. TechRxiv (2021). https://doi.org/10.36227/techrxiv.15091338.v1
3. P.L. Richards, The Josephson junction as a detector of microwave and far-infrared radiation, Chapter 6, in *Semiconductors and Semimetals*, vol. 12, ed. by R.K. Willardson, A.C. Beer (Elsevier, Amsterdam, 1977), pp. 395–440
4. Office of the Secretary of Defense (OSD), Small Business Technology Transfer (STTR) Program, Topic Number OSD21C-005 "Twisted graphene-based Josephson junction detectors," (2021).
5. G. Di Battista, P. Seifert, K. Watanabe, T. Taniguchi, K.C. Fong, A. Principi, D.K. Efetov, Revealing the thermal properties of superconducting magic-angle twisted bilayer graphene. Nano Lett. **22**, 6465–6470 (2022). https://doi.org/10.1021/acs.nanolett.1c04512
6. G.H. Lee, D.K. Efetov, W. Jung, L. Ranzani, E.D. Walsh, T.A. Ohki, T. Taniguchi, K. Watanabe, P. Kim, D. Englun, K.C. Fong, Graphene-based Josephson junction microwave bolometer. Nature **586**, 42 (2020). https://doi.org/10.1038/s41586-020-2752-4
7. R. Kokkoniemi, J.-P. Girard, D. Hazra, A. Laitinen, J. Govenius, R.E. Lake, I. Sallinen, V. Vesterinen, M. Partanen, J.Y. Tan, K.W. Chan, K.Y. Tan, P. Hakonen, M. Möttönen, Bolometer operating at the threshold for circuit quantum electrodynamics. Nature **586**, 47 (2020). https://doi.org/10.1038/s41586-020-2753-3
8. E.D. Walsh, W. Jung, G.-H. Lee, D.K. Efetov, B.-I. Wu, K.-F. Huang, T.A. Ohki, T. Taniguchi, K. Watanabe, P. Kim, D. Englund, K.C. Fong, Josephson junction infrared single-photon detector. Science **372**, 409 (2021). https://doi.org/10.1126/science.abf5539
9. E.D. Walsh, D.K. Efetov, G.-H. Lee, M. Heuck, J. Crossno, T.A. Ohki, P. Kim, D. Englund, K.C. Fong, Graphene-based josephson-junction single-photon detector. Phys. Rev. Appl. **8**, 024022 (2017). https://doi.org/10.1103/PhysRevApplied.8.024022
10. X. Du, D.E. Prober, H. Vora, C.B. Mckitterick, Graphene-based bolometers graphene. 2D Mater. **1**, 1 (2014). https://doi.org/10.2478/gpe-2014-0001
11. C.H. Bennett, G. Brassard, Quantum cryptography: public key distribution and coin tossing. Theor. Comp. Sci. **560**, 7 (2014). https://doi.org/10.1016/j.tcs.2014.05.025
12. J.M. Park, Y. Cao, L.Q. Xia, L.-Q. Xia, S. Sun, K. Watanabe, T. Taniguchi, P. Jarillo-Herrero, Robust superconductivity in magic-angle multilayer graphene family. Nat. Mater. **21**, 877 (2022). https://doi.org/10.1038/s41563-022-01287-1
13. F.J. González, G.D. Boreman, Comparison of dipole, bowtie, spiral and log-periodic IR antennas. Infrared Phys. & Technol. **46**, 418 (2005). https://doi.org/10.1016/j.infrared.2004.09.002
14. C.A. Balanis, *Antenna theory: analysis and design*, 3rd edn. (Wiley, Hoboken, NJ, 2005)
15. A.C. Gadelha, D.A.A. Ohlberg, F.C. Santana, G.S.N. Eliel, J.S. Lemos, V. Ornelas, D. Miranda, R.B. Nadas, K. Watanabe, T. Taniguchi, C. Rabelo, P. Paulo de Mello Venezuela, G. Medeiros-Ribeiro, A. Jorio, L.G. Cançado, L.C. Campos, Twisted bilayer graphene: a versatile fabrication method and the detection of variable nanometric strain caused by twist-angle disorder. ACS Appl. Nano Mater. **4**, 1858 (2021). https://doi.org/10.1021/acsanm.0c03230
16. H. Hashiba, V. Antonov, L. Kulik, A. Tzalenchuk, S. Komiyama, Sensing individual terahertz photons. Nanotechnology **23**, 165203 (2010). https://doi.org/10.1088/0957-4484/21/16/165203